DTIP 11-13 May 2011, Aix-en-Provence, France

A Methodology for the Pull-in Voltage of Clamped Diaphragms

Joseph Lardiès, Marc Berthillier
Institute FEMTO-ST; DMA; UMR CNRS 6174
Rue de l'Epitaphe
25000 Besançon, FRANCE

Abstract- **Due to the electrostatic excitation principle, MEMS based capacitive microphones exhibit a nonlinear behaviour and this communication investigates these nonlinearities with the aim to optimize the input voltage signal. The nonlinear electrostatic force due to the bias voltage is combined with the 2D load-deflection model of a square or circular diaphragm to evaluate the pull-in voltage. An analytical solution is derived to calculate the electrostatic pressure, the pull-in voltage and the deflection profile of the diaphragm. Numerical results with clamped square and circular diaphragms are presented showing the effectiveness of the method.**

I. INTRODUCTION

MEMS-based capacitive microphones offer advantages due to their small size, high sensibility, batch fabrication capability and low power consumption. A MEMS capacitive-type microphone is basically an electrostatic transducer converting electrical energy into mechanical energy and vice-versa. A good design requires a large displacement from the bias voltage for efficient energy coupling between the movable microplate or diaphragm and the air. The microplate can also be deflected by ambient pressure if the cavity beneath the microplate is vacuum sealed, which is necessary for immersion applications. However, optimum energy coupling is achieved when the plate is near the structural instability known as pull-in, where the largest stable plate deflection occurs. Beyond this point, the movable plate snaps onto the fixed plate (or substrate). Many resonance applications demand better understanding of MEMS behaviors, especially near the pull-in instability. Finite element method (FEM) simulations and analytical plate or membrane models have been used to analyze resonating microstructures effects. However, most FEM simulations are computationally inefficient or breakdown near pull-in of electrostatically actuated structures, and membrane model ignore plate bending, which is needed for bending dominate microstructures.

The central component in micro-electro-mechanical systems is the mechanical resonator which constitutes a capacitive transducer and is formed with two plates: a fixed plate and a movable plate. Due to the electrostatically force, when the gap between the two plates becomes two thirds of the initial gap, the movable plate is not stable, we have a ''push-down'' phenomenon and the MEMS fails. From the dynamics point of view, the system loses its stability and the gap being equal to two-thirds of the initial gap is termed the minimum gap in MEMS [1].

The electrostatic force associated with the voltage is non linear due to its inverse square relationship with the airgap thickness between the capacitor electrodes. This gives rise to the pull-in phenomenon that causes the movable structure (membrane) to collapse if the bias voltage exceeds the pull-in limit and limits the effective range of deformation of the structure. Accurate determination of the pull-in voltage, or the collapse voltage, is critical in the design process to determine the sensitivity, harmonic distortion and the dynamic range of a MEMS-based capacitive transducer. In [2] a method is provided to approximate pull-in voltage for cantilevers, fixed-fixed beams and circular diaphragms under electrostatic actuation in which the pull-in voltage depends on the undeformed gap and on the linear elastic response to an applied uniform load. In this communication an analytical solution is described to calculate the pull-in voltage and diaphragm deflection under electrostatic actuation, for square and circular diaphragms. The method incorporates both the nonlinearities of the electrostatic force and the large deflection model for a clamped square or circular diaphragm. The developed analytical method allows for a fast, more accurate determination of the developed electrostatic pressure, maximum diaphragm deflection for different bias voltage and the pull-in voltage. The method can easily be extended to the cases of cantilevers and fixed-fixed beams.

II. MODEL DEVELOPMENT

A. Parallel-Plate Approximation

A parallel plate approximation is first considered to highlight the major aspects of the analysis. A schematic cross section of a MEMS capacitive-type microphone is shown in Fig. 1. An external voltage V is applied between the upper and lower conductors, which causes the upper conductor to electrostatically deflect downwards. Deflection increases with voltage until pull-in is reached. A static displacement of the diaphragm of a capacitive cell due to the bias voltage is shown

 ISBN:978-2-35500-013-3

this figure.

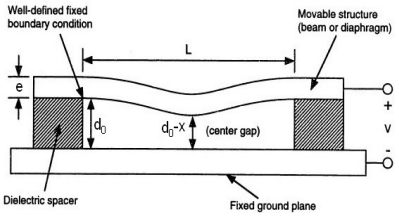

Fig. 1. Cross-section of a MEMS-based capacitive sensor.

We introduce a simplified one-dimensional (1-D) pull-in model in which the pull-in voltage depends on the undeformed gap and on the linear elastic response to an applied uniform load. While not numerically accurate, this model has the virtue of providing a functional form, which, for many structures, can be approximated analytically by solving a suitable linear equation. Fig.2 shows a lumped 1-D pull-in model, which provides some guidance in how the functional form is developed. The problem is approximated by a rigid body suspended by a lumped linear spring with spring constant *K*.

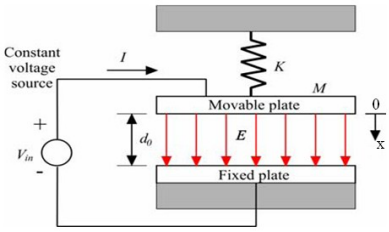

Fig. 2. A simplified mechanical model for a parallel-plate capacitor.

As shown in Fig. 2 the fixed plate of the capacitor with area *A* is connected with a constant supply voltage *V*. The other plate of the capacitor with mass *M* and area *A* is movable and rigid. The support of the moving plate is modeled through an equivalent spring with stiffness *K*. Without any electrostatic force, the gap between two plates of the capacitor in the MEMS is d_0 : it is the initial air gap. The coordinate *x* is shown in Fig. 2 and the origin is at equilibrium without any voltage. By applying a voltage across the plates, an electrostatic attractive force $F_e(x)$ is induced which leads to a decrease of the gap spacing, thereby stretching the spring. This results in an increase of the mechanical elastic force (or spring force) $F_m(x)$ which counteracts the electrostatic force. Pull-in instability occurs as a result of the fact that the electrostatic force increases non-linearly with decreasing gap spacing, whereas the mechanical elastic force is a linear function of the change in the gap spacing. In simple terms, the pull-in voltage can be defined as the voltage at which the restoring spring force can no longer balance the attractive electrostatic force. Our purpose is to determine this pull-in voltage.

B. First Order Analysis

Neglecting any damping within the system, the equation of motion of the movable plate due to an electrostatic attraction force $F_e(x)$ caused by a constant supply voltage *V* is:

$$M\frac{d^2x}{dt^2} + Kx = F_e(x) = \frac{\varepsilon_0 A V^2}{2(d_0 - x)^2} \quad (1)$$

The mechanical elastic force is $F_m(x) = Kx$ and ε_0 is the permittivity of the free space. At the static equilibrium the mechanical elastic force equals the electrostatic attraction force and the relationship between the voltage V and displacement of the movable plate is :

$$V=(d_0 - x)\sqrt{2Kx/(\varepsilon_0 A)} \quad (2)$$

The maximum of the voltage is obtained for $dV/dx=0$ and from this equation we obtain the distance where the pull-in occurs: $x_{pi} = d_0/3$ and the pull-in gap is $d_{pi} = 2d_0/3$. The pull-in voltage for this ideal parallel plate structure is then :

$$V_{pi} = \sqrt{8Kd_0^3/(27\varepsilon_0 A)} \quad (3)$$

and the spring constant of the movable plate is given by:

$$K = 27\varepsilon_0 A V_{pi}^3/(8 d_0^3) \quad (4)$$

If the applied voltage is increased beyond the pull-in voltage, the resulting electrostatic force will overcome the elastic restoring force and will cause the movable plate to collapse on the fixed plate and the capacitor will be short circuited.

To obtain stiffness due to the electrostatic force we expand (1) using a Taylor series approximation about the nominal distance x_0 :

$$M\frac{d^2x}{dt^2} + \left(K - \frac{\varepsilon_0 A V^2}{(d_0 - x_0)^3}\right)x = \frac{1}{2}\frac{\varepsilon_0 A V^2}{(d_0 - x_0)^2}\left[1 - \frac{2x_0}{(d_0 - x_0)}\sum_{n=3}^{N}\frac{n(x - x_0)^{n-1}}{(d_0 - x_0)^{n-1}}\right] \quad (5)$$

The electrostatic attraction force effectively modifies the spring constant *K* of the movable plate and the effective spring constant at a specified voltage *V* is :

$$K_{effective} = \left(K - \frac{\varepsilon_0 A V^2}{(d_0 - x_0)^3}\right) \quad (6)$$

The amount of modification is termed as spring softening and the resonant frequency of the structure is shifted from $\omega_{res}=\sqrt{K/M}$ to $\omega_{res}=\sqrt{K_{effective}/M}$.

The simple parallel-plate approximation method assumes that the beam has a linear spring constant, considers a piston like motion, and predicts that the pull-in when the highest deformation exceeds one-third of the gap. This analysis neglects the effects of the fringing field capacitances and

 ISBN:978-2-35500-013-3

excludes the nature of the fixed boundary conditions, non-uniformity of the electrostatic pressure, effects of the residual stress, and the developed nonlinear distribution due to the stretching of the beam. For wide beams with small airgaps, errors up to 20% have been reported in literature due to such approximations [2]. In the next section we analyze the case of a rigidly clamped square diaphragm separated from a rigid backplate by a small airgap.

III. SQUARE DIAPHRAGM ANALYSIS

A. Load-deflection characteristics of a square diaphragm

The load-deflection analysis has been developed for the measurement of the mechanical properties of thin films [3-5], and the deflection is measured as a function of applied pressure as shown in Fig. 3. In [3] and [4] the biaxial modulus and the residual stress of the film are extracted from the data using various mathematical models.

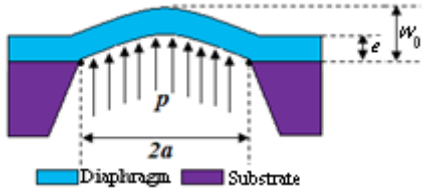

Fig. 3. Deflection of a square diaphragm in response to an applied pressure.

Due to the presence of residual stress and a significantly large deflection of the diaphragm compared to its thickness, the developed strain energy in the middle of the diaphragm causes a stretch of the diaphragm middle surface. The deflection of the diaphragm middle surface corresponds to a nonlinear behavior of a rigidly clamped diaphragm and is known as spring hardening. Thus, the analytical solution for diaphragm deflection from electrostatic forces must account for this spring hardening effect in addition to the nonlinear and non uniform electrostatic forces. Tabata et al. [3] developed an analytical solution for the load-deflection of membranes. They found a relationship between the external pressure load and the membrane deflection to determine the residual stress and Young's modulus of thin films. Pan et al. [4] compared the analytical solution with FEM analysis. They found that the functional form of the analytical results is correct, but some constants have to be corrected. Pan et al. also found that the analytical forms of the membrane's bending lines do not describe the real behavior very accurately. Maier-Schneider et al. [5] found an analytical solution for the load-deflection behavior of a membrane by minimization of the total potential energy. A new functional form of the membrane's bending shape was found which agrees well with experimental measurements and with FEM analysis.

Following the large deflection model, for a rigidly clamped square diaphragm with built-in residual stress, the load-deflection relationship of the midpoint of the diaphragm under a uniform pressure P can be expressed as [4-7] :

$$P(w_0) = C_1 \frac{e\sigma}{a^2} w_0 + C_2(\nu) \frac{eE}{a^4(1-\nu^2)} w_0^3 \qquad (7)$$

where P is the applied uniform pressure, w_0 the deflection of the diaphragm midpoint, e the diaphragm thickness, a half of the diaphragm side length, E the Young's modulus, ν the Poisson's ratio and σ the residual or internal stress. The dimensionless constants C_1 and C_2 are numerical parameters which are obtained from the results of Maier-Schneider et al. [5] :

$$C_1 = 3{,}45 \text{ and } C_2(\nu) = 1{,}994(1-0{,}271\nu)/(1-\nu) \qquad (8)$$

If the midpoint deflection w_0 is known, the deflection of the diaphragm from mid-side to mid-side can be calculated using [6-8] :

$$w(y,0) = w_0(1+0{,}401(y/a))^2 \cos(\pi y/2a) \qquad (9)$$

The 2-D distributed problem is approximated by a rigid body suspended by a lumped spring. The spring constant has units of N/m and is defined as $F_{elastic}/w_{Max}$ where w_{Max} is the maximum displacement of the diaphragm with no electrostatic load, but with a uniform distributed pressure load P. In our case we have: $w_{Max}=w_0$, $P=P(w_0)$ and $F_{elastic}=P(w_0)A$, so the nonlinear spring constant of the square diaphragm is :

$$K_{nl} = \frac{P(w_0)A}{w_0} = \left(C_1 \frac{e\sigma}{a^2} + C_2(\nu) \frac{eE}{a^4(1-\nu^2)} w_0^2\right) A \qquad (10)$$

The deflection-dependent nonlinearity due to spring hardening appears in equation (11) where the square of the midpoint deflection variable w_0 has been obtained. For a test device we consider the parameters given in table 1.

TABLE I
MODEL PARAMETERS

parameter	e	a	d_0	E	ν	σ
value	0,8	1,2	3,5	169	0,28	20
unity	µm	µm	µm	GPa	-	MPa

Spring hardening resulting from the deflection of a clamped square diaphragm midpoint due to an applied uniform pressure is plotted in Fig.4. From this figure we can obtain the value of the non-linear spring.

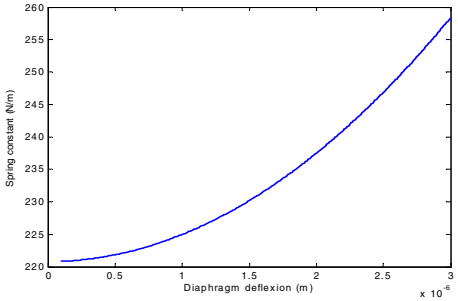

Fig. 4. Spring constant and diaphragm deflection

 ISBN:978-2-35500-013-3

B. *Pull-in voltage evaluation of a square diaphragm*

The analysis carried out in section 2 for a parallel plate capacitor structure can be extended to the case of a fully clamped square diaphragm separated from a rigid backplate by a small airgap. The deflection of the diaphragm is due to the resultant effect of electrostatic and restoring elastic forces (air damping force is neglected). For a parallel plate configuration (Fig. 2) the non linear electrostatic force is always uniform. However, for a rigidly clamped diaphragm, the electrostatic force becomes non-uniform due to a hemispherical deformation profile of the diaphragm. Thus, to evaluate the deflection of a rigidly clamped diaphragm under an electrostatic force, it is necessary to obtain a uniform linear model of the electrostatic force that can be applied in load-deflection equation (7). A uniform linearized model of the electrostatic force can be obtained from (5) by linearizing the electrostatic force about the zero deflection point $x_0 = 0$. The linearized electrostatic force is :

$$F_{elect.} = \varepsilon_0 V^2 \left(\frac{1}{2d_0^2} + \frac{x}{d_0^3} \right) A \qquad (11)$$

and the effective linearized uniform electrostatic pressure on the diaphragm is :

$$P_{elect.} = \frac{F_{elect.}}{A} = \varepsilon_0 V^2 \left(\frac{1}{2d_0^2} + \frac{x}{d_0^3} \right) \qquad (12)$$

This equation is general and can be applied to any sort of diaphragms. We deduce the pull-in electrostatic pressure by replacing x by the pull-in deflection $d_0/3$:

$$P_{PI\text{-}elect.} = \frac{5\,\varepsilon_0 V_{PI}^2}{6\,d_0^2} \qquad (13)$$

where V_{PI} represents the desired pull-in voltage. The applied uniform transverse pressure load of the rigidly clamped square diaphragm built in residual stress, obtained from elastic considerations (equation 7) equals the effective linearized uniform electrostatic pressure (equation 13) and at the distance where the pull-in occurs we obtain :

$$C_1 \frac{e\sigma}{a^2} \frac{d_0}{3} + C_2(\nu) \frac{eE}{a^4(1-\nu^2)} \left(\frac{d_0}{3} \right)^3 = \frac{5\,\varepsilon_0 V_{PI}^2}{6\,d_0^2} \qquad (14)$$

The above equation is solved and we obtain the expression for the pull-in voltage for a clamped square diaphragm under an electrostatic pressure:

$$V_{PI} = \frac{d_0}{a} \sqrt{\frac{6}{5\,\varepsilon_0} \left[C_1 e\sigma \frac{d_0}{3} + \frac{C_2(\nu)\, eE}{a^2(1-\nu^2)} \left(\frac{d_0}{3} \right)^3 \right]} \qquad (15)$$

The pull-in voltage can be calculated using equation (15). With the parameters given in table 1 we obtain a value of 17.45 volts. If we use equation (3), which corresponds to the ideal case of two parallel plates, we obtain V_{pi} = 15.02 volts, a value which is 2.43 volts smaller than the value obtained with the method proposed in this communication. The mid-side to mid-side deflection profiles of the clamped diaphragm for different voltages is shown in Fig.5.

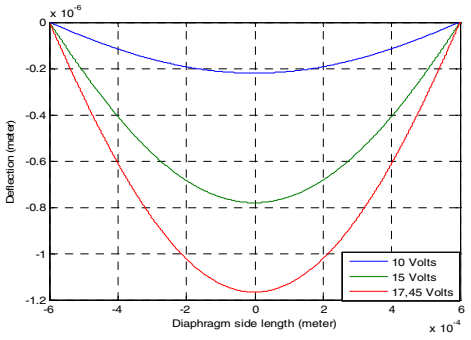

Fig. 5. Diaphragm deflection for different bias voltage

IV. CIRCULAR DIAPHRAGM ANALYSIS

A. *Load-deflection characteristics of a circular diaphragm*

Consider a circular plate of radius a and constant thickness e under a uniform transverse load $p_z = p_0$ and an initial tension load $N_r = N_0$, as shown in Fig.6.

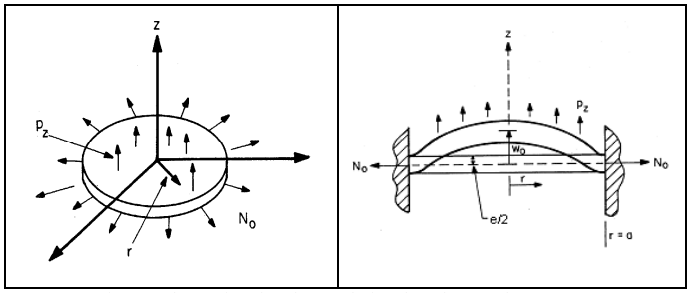

Fig.6. Schematic of a clamped circular plate under an initial in-plane stress N_0

Based on von Karman plate theory [6] for large circular plate deflections, the equilibrium equations for the symmetrical bending of this plate are :

$$(r\,N_{,r})_{,r} - N_\theta = 0 \qquad (16)$$

$$(r\,Q_r)_{,r} + (r\,N_r w_{,r})_{,r} + r\,p_0 = 0 \qquad (17)$$

$$r\,Q_r = (r\,M_r)_{,r} - M_\theta \qquad (18)$$

where $(\,)_{,r}$ indicates the differentiation with respect to the radial coordinate r, w is the normal displacement or the deflection of the plate in the z-direction, N_r , N_θ are the lateral loads, Q_r is the shear force, M_r and M_θ are the bending moments. The shear force can be obtained by integrating (17)

$$Q_r + N_r w_{,r} + \frac{1}{2} p_0 r = 0 \qquad (19)$$

 ISBN:978-2-35500-013-3

Using the radial and tangential midplane strains and curvatures [6] the second version of the shear force is :

$$Q_r = - D \left(w_{,rrr} + \frac{1}{r} w_{,rr} - \frac{1}{r^2} w_{,r} \right) \qquad (20)$$

where $D=Ee^3/12(1-\nu^2)$ is the flexural rigidity of the plate. Placing (20) into (19) produces:

$$w_{,rrr} + \frac{1}{r} w_{,rr} - \frac{1}{r^2} w_{,r} - \frac{N_r}{D} w_{,r} = \frac{p_0 r}{2D} \qquad (21)$$

The analytical solution of (21) is given by [9] :

$$w(r) = \frac{6Pe(1-\nu^2)}{k^2} \left[\frac{(I_0(kr/a) - I_0(k))}{k I_1(k)} + \frac{a^2 - r^2}{2a^2} \right] \qquad (22)$$

where $I_0(\ )$ and $I_1(\ )$ are the modified Bessel functions of the first kind [6], P is the nondimensional loading parameter and k is the nondimensional tension parameter. These two parameters are defined as:

$$P = \frac{p_0 a^4}{E e^4} \quad ; \quad k = a\sqrt{\frac{N_0}{D}} = \frac{a}{e}\sqrt{\frac{N_0 12(1-\nu^2)}{E e}} \qquad (23)$$

Two limiting cases are of interest here: the pure plate case where the tension parameter has the value $k=0$ and the pure membrane case where $k \to \infty$. For the pure plate case, taking the small argument limit of the modified Bessel functions, the corresponding deflection is:

$$w(r) = \frac{3}{16} e P (1-\nu^2) \left(1 - \left(\frac{r}{a}\right)^2\right)^2 \qquad (24)$$

For the pure membrane case, taking the large argument limit of the modified Bessel functions, the pure membrane deflection is:

$$w(r) = \frac{3e}{k^2} P (1-\nu^2) \left(1 - \left(\frac{r}{a}\right)^2\right) \qquad (25)$$

In Fig.7 the center deflection of the clamped circular plate, normalized by the transverse load, is plotted against the initial nondimensional tension parameter k. The effect of initial in-plane tension (or the lateral loads effect) is shown in this figure where two asymptotes are present. The horizontal part of the curve means the center deflection is in a linear proportion to the applied transverse load ($W(0) \propto P$, see also (24)) and is not a function of the initial tension, thus it reflects a plate behavior. The inclined straight line indicates a nonlinear variation of the center deflection with the tension parameter k ($W(0)/P \propto 1/k^2$, see also (36)), hence, a membrane behavior is revealed due to the nonlinearity of $W(0)/P$. In this Fig.7, there appears to be a transition from pure plate behavior to pure membrane behavior in the region from $k \approx 1$ to $k \approx 20$. For $k<1$ we have a plate behavior and for k>20 a membrane behavior dominates the majority of the clamped circular plate.

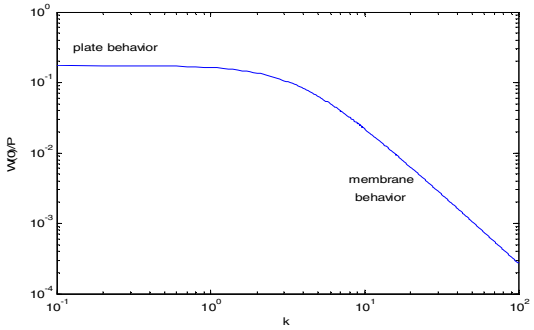

Fig.7 Center deflection normalized by the loading parameter as a function of the tension parameter

In order to have a thorough insight to the effects of initial tension upon the related geometrical responses, normalized deflection shapes are plotted in Fig.8. As the tension parameter k increases a sharp change in the curvature near the edge appears, in order to accommodate the zero slope boundary condition.

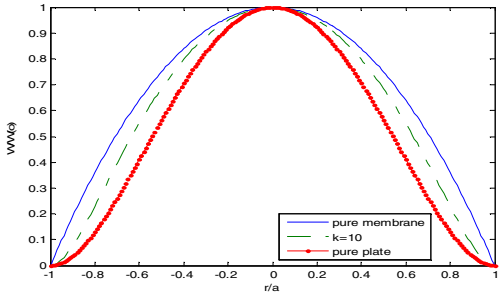

Fig. 8. Normalized deflection as a function of normalized radial distance

B. Pull-in voltage evaluation of a circular diaphragm

From equation (22) we deduce the uniform transverse pressure which is applied at the center of the clamped circular plate:

$$p_0 = \frac{2Dk^2 w(0)}{a^4} \left[\frac{1}{2} - \frac{I_0(k)}{k I_1(k)} \right]^{-1} \qquad (26)$$

As shown in paragraph II, we assume that the pull-in effect occurs when the deflection of the movable plate is one-third of the original air gap d_0 and the uniform pressure load given by (26) is equal to the pull-in electrostatic pression given by (13). We obtain:

$$\frac{2Dk^2}{a^4} \left(\frac{d_0}{3} \right) \left[\frac{1}{2} - \frac{I_0(k)}{k I_1(k)} \right]^{-1} = \frac{5 \varepsilon_0 V_{PI}^2}{6 d_0^2} \qquad (27)$$

 ISBN:978-2-35500-013-3

The above equation is solved and we obtain the expression for the pull-in voltage for a rigidly clamped circular plate:

$$V_{PI} = \frac{2k\,d_0}{a^2}\sqrt{\frac{D\,d_0}{5\,\varepsilon_0}\left[\frac{1}{2} - \frac{I_0(k)}{kI_1(k)}\right]^{-1}} \qquad (28)$$

In the case of a pure circular plate the uniform transverse pressure is obtained from (24):

$$p_0 = \frac{64\,D\,w(0)}{a^4} \qquad (29)$$

and at one-third of the original air gap we obtain the pull-in voltage for a pure clamped circular plate:

$$\frac{64\,D}{a^4}\left(\frac{d_0}{3}\right) = \frac{5\,\varepsilon_0\,V_{PI}^2}{6\,d_0^2} \Rightarrow V_{PI} = \frac{8\,d_0}{a^2}\sqrt{\frac{2\,D\,d_0}{5\,\varepsilon_0}} \qquad (30)$$

In the case of a pure circular membrane the uniform transverse pressure is obtained from (25):

$$p_0 = \frac{4\,D\,k^2\,w(0)}{a^4} \qquad (31)$$

and at one-third of the original air gap we obtain the pull-in voltage for a pure clamped circular membrane:

$$\frac{4\,D\,k^2}{a^4}\left(\frac{d_0}{3}\right) = \frac{5\,\varepsilon_0\,V_{PI}^2}{6\,d_0^2} \Rightarrow V_{PI} = \frac{k\,d_0}{a^2}\sqrt{\frac{8\,D\,d_0}{5\,\varepsilon_0}} \qquad (32)$$

To illustrate the above model of pull-in evaluation, a clamped circular diaphragm of Young's modulus E = 169 GPa and Poisson's ratio ν = 0,28 is considered. The thickness of the plate is e = 0,8 µm and the airgap thickness is d_0 = 3,5 µm. The permittivity in free space is ε_0 = 8,5x10^{-12} F.m^{-1} and the residual in-plane stress is $\sigma_0 = N_0/e$ = 20 MPa. Fig. 7 shows the pull-in voltage for a plate having the previously device parameters and for a pure membrane as a function of radius. It is evident that there is negligible difference between the pull-in voltage evaluated using a pure membrane model and given by (32) and the pull-in voltage our circular clamped plate.

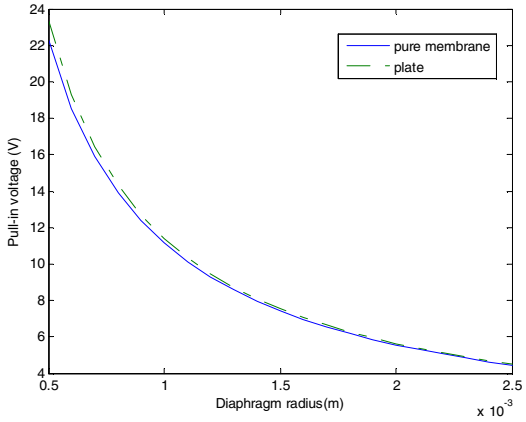

Fig. 9. Pull-in voltage for a pure circular membrane and for a circular plate

V. CONCLUSION

The deflections of clamped square and circular plates under a uniform transverse load and in-plane tension loads have been studied in the communication. In particular the transition from plate behavior to membrane behavior has been described for a clamped circular plate. A new relatively simple closed-form model to evaluate the pull-in voltage associated with rigidly clamped diaphragms subject to an electrostatic force has been presented and numerical results have been obtained showing the effectiveness of the method in pull-in voltage evaluation.

REFERENCES

[1] S. D. Senturia, *Microsystem Design*. Springer, 2000.

[2] P.O. Osterberg and S.D. Senturia, ''M-Test: a test chip for MEMS material property measurements using electrostatically actuated test structures'', *J. of Microelectromechanical Systems*, Vol. 6, pp.107-117, 1997.

[3] O. Tabata, K. Kawahata, S. Suguyama and I. Igarashi, ''Mechanical property measurements of thin films using load-deflection of composite rectangular membranes'', *Sensors and Actuators*, Vol. 20, pp. 135-141, 1989.

[4] J.Y. Pan, P. Lin, F. Maseeh, S.D. Senturia, ''Verification of FEM analysis of load-deflection methods for measuring mechanical properties of thin films'', *IEEE Solid-State Sensors and Actuators Worshop*, Hilton Head Island, pp. 70-73, 1990.

[5] D. Maier-Schneider, J. Maibach and E. Obermeier, ''A new analytical solution for the load-deflection of square membranes'', *J. of Microelectromechanical Systems,* Vol. 4, pp. 238-241, 1995.

[6] S. Timoshenko, *Theory of Plates and Shells*. Mc Graw Hill, 1959.

[7] S. Chowdhury, M. Ahmadi and W.C. Miller, ''Nonlinear effects in MEMS capacitive microphone design'', *International Conference on MEMS, NANO and Smart Systems 03*, Banff, Alberta, Canada, 2003.

[8] J. Lardiès, O. Arbey and M. Berthillier, ''Analysis of the pull-in voltage in capacitive mechanical sensors'', *Third International Conference on Multidisciplinary Design Optimization and Applications*, 21-23 June 2010, Paris.

[9] M Sheplak and J. Dugundji, ''Large deflections of clamped circular plates under initial tension'', *J. of Applied Mechanics*, Vol. 65, pp.107-115, 1998.

 ISBN:978-2-35500-013-3